Reactions of Laser-Ablated Aluminum Atoms with Ammonia. Infrared Spectra of $HAlNH_2$, $AlNH_2$, and HAlNH in Solid Argon

Dominick V. Lanzisera and Lester Andrews*

Department of Chemistry, University of Virginia, Charlottesville, Virginia 22901

Received: February 13, 1997; In Final Form: April 4, 1997[⊗]

Pulsed laser-ablated Al atoms react with NH_3 to give two major products, $HAlNH_2$ and $AlNH_2$, which are trapped in solid argon and identified from infrared spectra through isotopic substitution (^{15}N, D) and MP2 calculations of product structures and isotopic frequencies. The bent HAlNH molecule was a minor product.

Introduction

Interest in III−V compounds arises largely for two reasons: the promise of new semiconductors and high-energy molecules and the comparison with isoelectronic organic compounds having multiple bonds.[1] Previously, boron−nitrogen compounds have been studied using matrix isolation following reaction of laser-ablated boron atoms with nitrogen,[2,3] ammonia,[4,5] and methylamines.[6] In the ammonia experiments, the linear product HBNH was characterized and compared to the isoelectronic HCCH molecule. Methyl-substituted iminoboranes—CH_3BNH, CH_3NBH, and CH_3BNCH_3—were identified in the methylamine experiments and contrasted with mono- and dimethylacetylene. In each of these molecules, among other similarities with the organic compounds, there is a formal triple bond between boron and nitrogen.

Besides boron−nitrogen compounds, other III−V combinations have drawn interest, such as theoretical calculations on B−P and Al−N systems[1,7,8] and EPR studies of aluminum−ammonia cocondensation products.[9] Davy and Jaffrey performed *ab initio* molecular electronic structure calculations to determine geometries, energies, and vibrational frequencies of compounds with the formula $AlNH_x$ ($x = 2-4$).[1] Their methods included Hartree−Fock configuration interaction with single and double excitations (CISD) for $AlNH_3$ and $AlNH_4$ and these two methods plus coupled cluster expansion (CCSD) for $AlNH_2$ isomers.

This article presents experimental evidence for Al−N−H compounds and supporting calculations which, despite being undertaken at a lower level of theory, are still quite close to both those of Davy and Jaffrey and the experimental vibrational frequencies. Isotopic frequencies for both deuterium and nitrogen-15 are also given for a variety of isomers. The main goal of this work is the identification of new product species and the comparison of experimental isotopic vibrational frequencies with calculated frequencies.

Experimental Section

Previous articles have described the apparatus for pulsed laser ablation, matrix isolation, and FTIR spectroscopy.[4−6] Mixtures of NH_3 in Ar (1:100−200) codeposited at 3 mmol/h for 1−2 h onto a 6−7 K cesium iodide window react with aluminum atoms ablated from a target source (Al, Aesar, 99.998% Puratronic) rotating at 1 rpm. The fundamental 1064 nm beam of a Nd:YAG laser (Spectra Physics DCR-11) operating at 10 Hz and focused with a +10 cm focal length lens ablated the target using 20−30 mJ per 10 ns pulse. The aluminum target was mechanically filed prior to insertion in the vacuum system to remove oxides from the surface. Following deposition, a Nicolet 550 Fourier transform infrared (FTIR) spectrometer collected spectra from 400−4000 cm^{-1} using a liquid nitrogen-cooled MCT detector with 0.5 cm^{-1} resolution and peak accuracy of ±0.2 cm^{-1}.

Reagent gases included NH_3 (Matheson), $^{15}NH_3$ (MSD Isotopes, 99% ^{15}N), and ND_3 (MSD Isotopes, 99% D). Prior to the first experiment, NH_3 was placed into the gas manifold and allowed to passivate the stainless steel walls. Then, NH_3 experiments were run by mixing a fresh sample of NH_3 with argon and flowing the gas mixture through a needle valve and deposition line. For $^{15}NH_3$ enrichment, the manifold was passivated with $^{15}NH_3$ for 18 h, which gave approximately 3:1 ^{15}N:^{14}N ratios. For the ND_3 experiments, only a small section of the NH_3 deposition line was used for argon mixed with ND_3, flowing through another needle valve near the reaction chamber, which gave approximately 90% deuteration of the reactant gas. For experiments with scrambled hydrogen isotopes, ND_3 was placed in the manifold, previously passivated with NH_3, and the four precursors NH_3, NH_2D, NHD_2, and ND_3 were present in these experiments with a H/D ratio of approximately 1/2.

After sample deposition, annealing to 15 K followed by broad-band mercury arc photolysis (Philips 175 W) was done to produce changes in the FTIR spectra. Further annealings to 25 and 35 K also changed some of the spectral features and allowed bands behaving similarly to be grouped together. Annealing behavior among absorptions of different products was more distinct than photolysis behavior and, therefore, a better diagnostic.

We performed Hartree−Fock (HF) calculations on potential product molecules using the Gaussian 94 program package.[10] For all calculations, a Møller−Plesset correlation energy correction followed the HF calculation and was truncated at second order (MP2 method).[11] The basis set for each atom was the Dunning/Huzinaga full double zeta with one single first polarization function (D95*).[12] The geometry optimizations used redundant internal coordinates and converged via the Berny optimization algorithm,[10,13] and the program calculated vibrational frequencies analytically. For HAlN and HNAl, imaginary vibrational frequencies were calculated for the bending mode, and further calculations using density functional theory with the B3LYP functional[14] and 6-311G* basis set[15] obtained satisfactory vibrational frequencies.

Results

Matrix infrared spectra of the reaction products using various ammonia isotopic combinations are reported. The relative

[⊗] Abstract published in *Advance ACS Abstracts,* June 15, 1997.

S1089-5639(97)00560-4 CCC: $14.00

TABLE 1: Observed Frequencies (cm^{-1}) and Annealing Behavior for Products in the Al + NH_3 Reactions

$^{14}NH_3$	$^{15}NH_3$	ND_3	mixed H/D[a]	25 K[b]	35 K[b]	identity
3495.0	3486.6			+10	−50	$AlNH_2$ site
3486.2	3477.4			−30	−35	$AlNH_2$
3476.8	3468.0			+10	−30	$AlNH_2$ site
3125.7	3119.1			+20	−35	NH
1958.4	1958.4	1436.1		−15	−40	?
1899.5	1899.5	1384.3		0	0	HAlNH
1890.9	1890.9	1386.4		+10	−30	HAlNH site
1887.8	1887.8			+40	−20	HAlNH site
1800.6	1800.6	1799.4		+4300	+120	?
1799.2	1799.2	1797.9		+4300	+120	?
1761.7	1761.7	1282.7		−10	−30	$HAlNH_2$
1739.8	1739.8	1269.4		+100	+90	$HAlNH_2$ site
1590.7	1590.7	1157.4		+5	−40	AlH
1541	1537			−15	−10	$Al(NH_2)_2$
1537.7	1532.8	1149.4		−10	−65	$AlNH_2$ site
1533.5	1531.4	1147.2		−10	0	$AlNH_2$ site
1524.9	1521.7	1151.4	1366?	−10	−30	$HAlNH_2$
1520.3	1514.7	1137.8	1343.8	−30	−35	$AlNH_2$
1494.8	1490.9	1106.7	1316.3	−20	−20	NH_2
1282.5	1281.1, 1279.8			−60	−35	HNNH
836.1	830.6, 824.3			+65	−100	$Al(NH)_2$ site
833.1	827.2, 821.4			−15	−20	$Al(NH)_2$
785.3	770.8			+30	−80	$HAlNH_2$ site
778.7	766.9	748.3	749.2?	−10	−30	$HAlNH_2$
747.7	742.3, 737.5			−15	−10	$Al(NH_2)_2$
734.6	723.9	710.2	721	+135	+60	$AlNH_2$ site
730.9	718.0	706.3	716.9	−15	−70	$AlNH_2$ site
726.3	713.3	694.8	713.1	−30	−35	$AlNH_2$
707.6	703.9	550.7		−55	−70	$HAlNH_2$ site
704.6	700.9	549.8	655.5, 651.1, 644.2, 580.2, 575.0	−10	−30	$HAlNH_2$
702.0	698.1	548.0		+135	−100	$HAlNH_2$ site
530.6	530.5		495.5, 489.6	0	0	HAlNH
406.7	403.7			−30	−35	$AlNH_2$

[a] Product peaks in the mixed H/D experiment that are not present or present in only trace amounts in either the NH_2 or ND_3 experiments. [b] Percent change in intensity of the peak following annealing to the given temperature.

increase or decrease of the peak intensities upon photolysis and annealing helps to assign peaks of different isotopes and peaks of different vibrational modes to the same product. Because ^{27}Al is the only naturally occurring isotope of aluminum, all of the isotopic data arises from the ammonia reactant gas. Distinguishing products containing aluminum from ammonia fragments is aided by previous experiments with boron and ammonia. Other than aluminum−nitrogen−hydrogen species and photolysis products, aluminum oxides such as AlOAl and OAlO arise because of oxides on the aluminum target surface,[16] but these peaks are too weak to obscure any of the reaction products.

Al + NH_3. Table 1 lists frequencies and annealing behavior of four isotopic ammonia experiments with aluminum. Figure 1a displays a spectrum in the 850−680 cm^{-1} range for the best NH_3 experiment, using a 1% NH_3 in Ar mixture and the high end of the laser power range. Reducing the concentration to 0.5% decreased product yield without significantly reducing the relative concentration of ammonia clusters while reducing the laser power provided significantly lower yield without any new information. The strongest absorption in this spectrum, at 704.6 cm^{-1} (labeled $HAlNH_2$), has two site splittings at 707.6 and 702.0 cm^{-1}. Upon photolysis, these absorptions increase 35%. Further annealing to 25 K strongly increases the 702.0 cm^{-1} site at the expense of intensity in the 707.6 cm^{-1} absorption, while keeping the main peak at nearly the same intensity. Annealing to 35 K afterward reduces the 704.6 cm^{-1} peak by 30% and nearly destroys both matrix sites. To the blue of this absorption lies a peak at 726.3 cm^{-1} (labeled $AlNH_2$) with matrix sites at 730.9 and 734.6 cm^{-1}. The 726.3 cm^{-1} band increases 40% upon photolysis, and then declines 30% on annealing to 25 K and 35% more on 35 K annealing. A peak

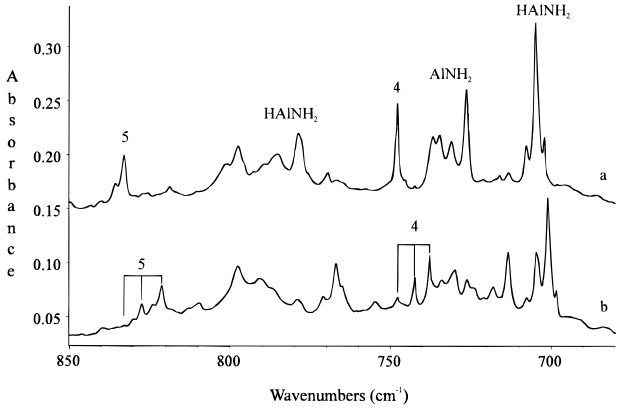

Figure 1. Infrared spectra in the 850−680 cm^{-1} region following pulsed laser ablation of Al atoms codeposited with Ar/NH_3 (100/1) samples on a CsI window at 6−7 K: (a) Al + $^{14}NH_3$ and (b) Al + $^{15}NH_3/^{14}NH_3$ (3/1). Peak labels are explained in the text.

at 747.7 cm^{-1} (labeled 4) develops a shoulder peak at 748.3 cm^{-1} upon photolysis, and the doublet is maintained throughout annealing. An absorption at 778.7 cm^{-1} (labeled $HAlNH_2$) grows on photolysis and 25 K annealing until almost disappearing on 35 K annealing. Finally, an absorption at 833.1 cm^{-1} (labeled 5) grows upon 25 K annealing and then disappears on further annealing to 35 K.

Figure 2a presents the spectrum for this experiment in the 1600−1480 cm^{-1} range. A strong AlH peak at 1590.7 cm^{-1} and the NH_2 band at 1494.8 cm^{-1} are observed.[5,17,18] Between these absorptions appear new product peaks. The strongest new band, at 1520.3 cm^{-1} (labeled $AlNH_2$), increases 40% on photolysis and then decreases following both annealings. The nearby absorption at 1524.9 cm^{-1} (labeled $HAlNH_2$) increases

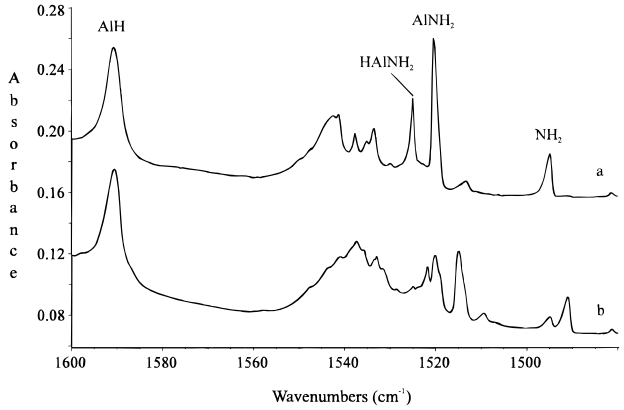

Figure 2. Infrared spectra in the 1600−1480 cm^{-1} region following pulsed laser ablation of Al atoms codeposited with Ar/NH_3 (100/1) samples on a CsI window at 6−7 K: (a) Al + $^{14}NH_3$ and (b) Al + $^{15}NH_3/^{14}NH_3$ (3/1). Peak labels are explained in the text.

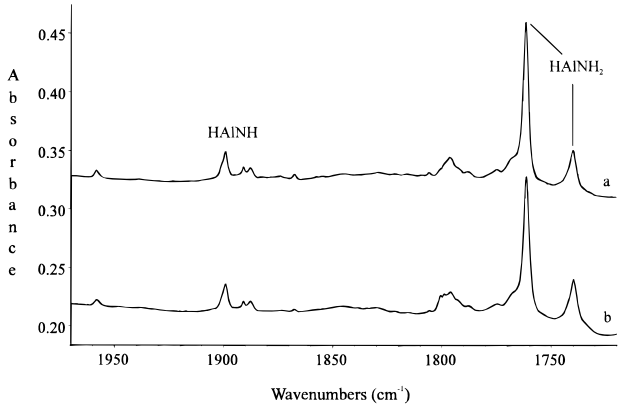

Figure 3. Infrared spectra in the 1970−1720 cm^{-1} region following pulsed laser ablation of Al atoms codeposited with Ar/NH_3 (100/1) samples on a CsI window at 6−7 K: (a) Al + $^{14}NH_3$ and (b) Al + $^{15}NH_3/^{14}NH_3$ (3/1). Peak labels are explained in the text.

35% on photolysis and following annealing to 35 K is actually larger than the 1520.3 cm^{-1} peak. The other absorptions in this region overlap, but sharp features at 1537.7 and 1533.5 cm^{-1} can be observed, as well as a broad absorption near 1541.3 cm^{-1}.

In the Al−H stretching region from 1970 to 1720 cm^{-1} (Figure 3a), the dominant peak at 1761.7 cm^{-1} (labeled $HAlNH_2$) increases 35% on photolysis and then diminishes 10 and 30% on annealing to 25 and 35 K, respectively. Nearby, a peak at 1739.8 cm^{-1} declines by 50% on photolysis and then grows 100% on annealing to 25 K and another 90% at 35 K. At 1899.5 cm^{-1}, a peak (labeled HAlNH) increases 50% on photolysis and remains virtually unchanged at 25 and 35 K. A weak absorption at 1958.4 cm^{-1} decreases 65% on photolysis, distinguishing it from the vast majority of peaks that show increased intensity. Finally, a broad absorption near 1800 cm^{-1} increases slightly on photolysis, but upon annealing to 25 K develops into a strong doublet about 60% of the size of the strong 1761.2 cm^{-1} band. This doublet, at 1800.6 and 1799.2 cm^{-1}, grows by 120% upon annealing to 35 K and is unlike any other band in the experiment.

In the N−H stretching region, only one distinct set of new bands can be seen amid the interference from ammonia absorptions. The peak at 3486.2 cm^{-1} has two site absorptions at 3495.0 and 3476.8 cm^{-1}, and these peaks grow 40% on photolysis and decrease sharply on annealing. A weak NH band[15,18] was observed at 3125.7 cm^{-1}. All other absorptions in this region are due to ammonia and ammonia clusters.[19]

Near the low-frequency limit of the spectrum, there is a weak absorption at 530.6 cm^{-1}, which increases 55% on photolysis and also increases on annealing. A noisy absorption at 406.7 cm^{-1} was also detected.

Al + $^{15}NH_3$. Figure 1b displays the spectrum of a $^{15}NH_3$ experiment run under approximately the same concentration and laser power as for the $^{14}NH_3$ spectrum in Figure 1a. Because the enrichment of $^{15}NH_3$ was only 75% due to exchange in the vacuum manifold, products from both isotopic reactants are observed. For example, a strong absorption at 700.9 cm^{-1} is more than twice as intense as the band near 703.9 cm^{-1} and behaves similarly upon photolysis and annealing; both the absorption at 704.6 cm^{-1} from residual $^{14}NH_3$ and the characteristic blue matrix site of the $^{15}NH_3$ 700.9 cm^{-1} band contribute to the intensity of this broader peak. The strong band at 713.3 cm^{-1} tracks with the 726.3 cm^{-1} band from the $^{14}NH_3$ experiment. An absorption at 766.9 cm^{-1} with a matrix site at 770.8 cm^{-1} matches the 778.7/785.3 cm^{-1} combination for $^{14}NH_3$, including sharp development of the site upon 25 K annealing followed by near destruction at 35 K. Two sharp new bands at 737.5 and 742.3 cm^{-1} behave similarly to each other and to the 747.7 cm^{-1} band from the $^{14}NH_3$ experiment. These spectra, then, suggest a product with two equivalent nitrogen atoms. Similarly, peaks at 821.4 and 827.2 cm^{-1} (with matrix sites at 824.3 and 830.6 cm^{-1}, respectively) form a nitrogen isotopic triplet with the 833.1 and 836.1 cm^{-1} absorptions for $^{14}NH_3$.

In Figure 2b, the AlH absorption remains at 1590.7 cm^{-1}, but the NH_2 peak shifts to 1490.9 cm^{-1}. Among the new bands, there is a nitrogen isotopic doublet at 1514.7 and 1520.3 cm^{-1}, while a band at 1521.7 cm^{-1} corresponds to the 1524.9 cm^{-1} band in the $^{14}NH_3$ experiment. Unfortunately, the cluster of peaks near 1535.0 cm^{-1} is further complicated by contributions from both ^{14}N and ^{15}N species, but absorptions at 1532.8 and 1531.4 cm^{-1} can be discerned.

In the Al−H stretching region (Figure 3b), there is no noticeable change in the frequencies for any of the peaks in the $^{15}NH_3$ experiments. Therefore, there is no nitrogen coupling to these stretching modes, as expected, because of the heavy mass of aluminum relative to nitrogen.

The N−H stretching region provides counterparts to peaks from the $^{14}NH_3$ experiments. The main peak, at 3477.4 cm^{-1}, has sites at 3486.6 and 3468.0 cm^{-1}, although overlap with ^{14}N peaks may obscure the precise location of these sites.

As in the $^{14}NH_3$ experiments, there are two absorptions near the low-frequency limit. An absorption at 530.5 cm^{-1} shifts only 0.1 cm^{-1} from the ^{14}N counterpart and exhibits the same photolysis and annealing dependence. Similarly, a peak at 403.7 cm^{-1} appears to track with the 406.7 cm^{-1} ^{14}N absorption, although the low signal-to-noise ratio in this region makes determining photolysis and annealing behavior somewhat problematic.

Al + ND_3. Figure 4c displays the best Al + ND_3 experiment in the 850−540 cm^{-1} region, and the higher frequency half of the spectrum is dominated by strong ND_3 and weaker NHD_2 precursor absorptions. Among the new peaks is a sharp absorption at 694.8 cm^{-1} (labeled $AlND_2$) which shows the same photolysis and annealing behavior as the 726.3 cm^{-1} band from the NH_3 experiments. Matrix sites at 706.3 and 710.2 cm^{-1} match the 730.9 and 734.6 cm^{-1} sites from NH_3 experiments. The strongest new absorption at 549.8 cm^{-1} (labeled $DAlND_2$) and evidence of small matrix sites to the blue and the red of this absorption, in addition to similar photolysis and annealing behavior, make this peak the deuterated counterpart of the 704.6 cm^{-1} peak in Figure 4a from the Al + NH_3 experiment. An

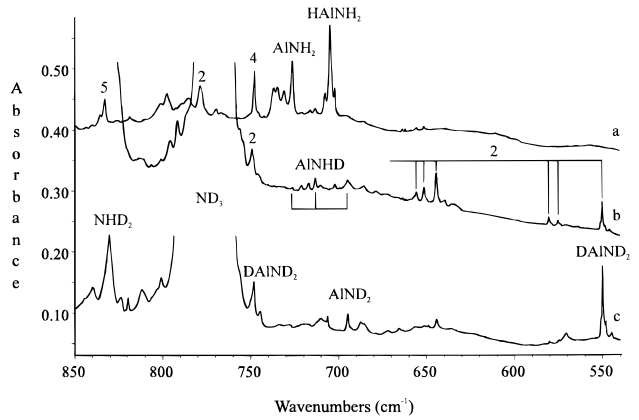

Figure 4. Infrared spectra in the 850−540 cm^{-1} region following pulsed laser ablation of Al atoms codeposited with Ar/NH_3 (100/1) samples on a CsI window at 6−7 K: (a) Al + NH_3, (b) Al + NH_3/NH_2D/NHD_2/ND_3, and (c) Al + ND_3. Peak labels are explained in the text. Note that the large ND_3 absorptions in (b) and (c), as well as the NHD_2 absorption in (b), have been pared to increase the clarity of (a).

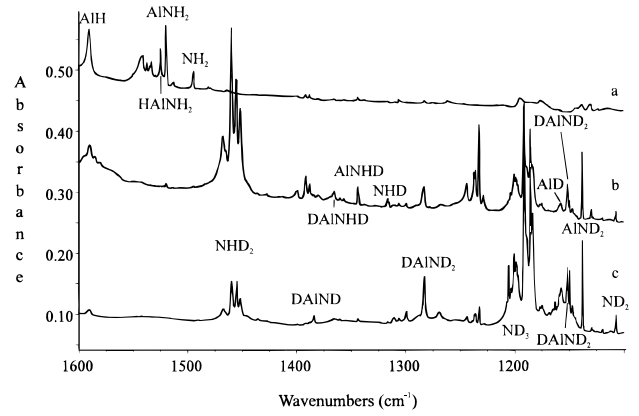

Figure 5. Infrared spectra in the 1600−1100 cm^{-1} region following pulsed laser ablation of Al atoms codeposited with Ar/NH_3 (100/1) samples on a CsI window at 6−7 K: (a) Al + NH_3, (b) Al + NH_3/NH_2D/NHD_2/ND_3, and (c) Al + ND_3. Peak labels are explained in the text.

absorption at 748.3 cm^{-1} (labeled $DAlND_2$) with a blue shoulder similarly matches the 778.8 cm^{-1} peak from NH_3.

The ND_3 absorptions are less of a problem in Figure 5c, from 1600 to 1100 cm^{-1}. Very little AlH is formed, but an AlD peak at 1157.4 cm^{-1} is clearly evident, as is ND_2 at 1106.7 cm^{-1}. The sharpest of the new absorptions at 1137.8 cm^{-1} (labeled $AlND_2$) increases 40% on photolysis and decreases on annealing, making it the ideal partner for the 1520.3 cm^{-1} peak in Figure 5a from the Al + NH_3 experiment. Between the 1137.8 cm^{-1} absorption and the AlD band are peaks at 1147.2, 1149.4, and 1151.4 cm^{-1}. These bands increase 20, 55, and 35%, respectively, on photolysis, and the annealing behavior is listed in Table 1. Of these bands, the 1151.4 cm^{-1} band (labeled $DAlND_2$) tracks best with the 1524.9 cm^{-1} absorption from the NH_3 experiments.

Al + NH_3/NH_2D/NHD_2/ND_3. Mixed H/D experiments provided all four possible ammonia isotopic combinations, with more deuterium than hydrogen in the present sample as NHD_2 had the strongest precursor. In Figure 4b, some peaks arise that also are present in the ND_3 spectrum, but several new peaks arise as well. The 549.8 cm^{-1} absorption is smaller than in the ND_3 experiment but is accompanied by a larger band at 644.2 cm^{-1}, a peak present with much less intensity in the ND_3 experiments. Peaks at 575.0, 580.2, and 651.1 cm^{-1} can also be detected in the ND_3 experiments but are much larger in the mixed H/D spectrum. The 651.1 cm^{-1} peak and a peak at 655.5 cm^{-1} can be detected in the NH_3 spectrum (Figure 4a), but again they are much larger in the mixed experiment. These five intermediate peaks (labeled 2) track with the 704.6/549.8 cm^{-1} NH_3/ND_3 pairing, as each develops a strong matrix site to the red upon 25 K annealing. These absorptions, then, are evidence that this product has at least three hydrogen atoms. The absence of a detectable absorption at 704.6 cm^{-1} confirms this hypothesis. The presence of these intermediates in Figure 4c is caused by incomplete deuteration of the manifold for these experiments, while the presence of a trace amount of deuterium in the NH_3 experiments is caused by incomplete passivation of the manifold with NH_3 following previous deuterated experiments.

Also in Figure 4b, there is a reasonably strong new absorption at 713.1 cm^{-1} with sites at 716.9 and 721.0 cm^{-1}. The main absorption tracks with those at 726.3 and 694.8 cm^{-1} in Figure 4a,c and suggests a product with two equivalent hydrogens. Note that weak absorptions at 726.3 and 694.8 cm^{-1} are present in Figure 4b. Also in this spectrum is a band at 749.2 cm^{-1}, which is very near the 748.3 cm^{-1} band in Figure 4c.

In Figure 5b, the new absorptions from the ND_3 experiments appear with less intensity, and there are a few new peaks. The NHD band at 1316.3 cm^{-1} is one such band. Nearby, a larger peak (labeled AlNHD) at 1343.8 cm^{-1} tracks with the 1520.3/1137.8 cm^{-1} bands from the NH_3 and ND_3 experiments. A few peaks near 1366 cm^{-1} appear to track with the 1524.9/1151.4 cm^{-1} bands and may correspond to a NH_2 mode with two inequivalent H atoms.

In the lower frequency region, the ND_3 experiments provide no new absorptions, but the mixed H/D experiments yield new peaks at 495.5 and 489.6 cm^{-1}. These bands track the NH_3 absorption at 530.6 cm^{-1} and indicate that the fully deuterated counterpart of this product may absorb near or below 400 cm^{-1}.

Calculations. Table 2 presents the results of MP2 calculations on potential product molecules, including geometric and frequency data. In the next section, there is discussion of our calculations relative to the more sophisticated ones by Davy and Jaffrey in the context of the specific molecules. For HNAl and HAlN, we obtained imaginary frequencies for the degenerate bending mode and repeated the calculations using DFT/B3LYP and obtained satisfactory geometries and frequencies, which are presented in Table 2.

Discussion

Identification of products makes use of isotopic vibrational frequency shifts involving nitrogen and hydrogen and calculations of energies and vibrational frequencies of potential product molecules. While the calculations of Davy and Jaffrey are higher level than the MP2 calculations presented in this article, our results agree quite well and provide isotopic data and oscillator strengths to help in the identification process.

Species 1: $AlNH_2$. Davy and Jaffrey predict that $AlNH_2$ is planar with two equivalent hydrogens and much more stable than its other isomers, H_2AlN and HAlNH.[1] The present MP2 calculations agree (Table 2) and suggest that there should be a strong Al−N stretching mode near 750 cm^{-1}. Table 3 presents experimental and calculated evidence for the presence of $AlNH_2$. The observed peak in NH_3 experiments at 726.3 cm^{-1} is assigned to the Al−N stretch, especially considering the ^{15}N peak shifts to 713.3 cm^{-1}. The nitrogen isotopic 14/15 ratio in the experiment, 1.018 23, closely matches our calculated ratio of 1.018 45. Given the identical photolysis and annealing behavior, the peak at 694.8 cm^{-1} must also be due to $AlND_2$, also in good agreement with calculations. Because this molecule has two equivalent hydrogen atoms, there should be a single

TABLE 2: SCF Energies, Geometries, and Vibrational Frequencies for H/Al/N Species Calculated Using the MP2 Method

species	energy (au)	bond lengths (Å)	bond angles (deg)	selected frequencies (intensities) for natural isotopes (cm^{-1} and km/mol))
$Al(NH_2)_2$	−353.162 73	$r_{AlN} = 1.83$; $r_{NH} = 1.02$	$\angle_{NAlN} = 122.7$; $\angle_{HNAl} = 119.7$; $\angle_{HNH} = 107.6$	3657.1 (45), 1622.0 (118), 806.8 (122), 386.9 (415)
$Al(NH)_2$	−351.890 26	$r_{AlN} = 1.66$; $r_{NH} = 1.01$	$\angle_{NAlN} = 180.0$; $\angle_{HNAl} = 180.0$	3783.3 (916), 905.3 (3614)
H_2AlNH_2	−298.710 69	$r_{AlH} = 1.58$; $r_{AlN} = 1.78$; $r_{NH} = 1.02$	$\angle_{NAlN} = 118.1$; $\angle_{HAlH} = 123.9$; $\angle_{HNAl} = 124.9$; $\angle_{HNH} = 110.3$	2005.4 (212), 838.4 (203), 780.2 (149), 639.0 (163), 470.7 (312)
$HAlNH_2$	−298.102 20	$r_{AlH} = 1.60$; $r_{AlN} = 1.79$; $r_{NH} = 1.02$[a]	$\angle_{NAlN} = 116.3$; $\angle_{HNH} = 110.3$; $\angle_{AlNH} = 124.4, 125.3$	1910.3 (151), 1626.4 (47), 808.1 (91), 765.7 (125), 439.4 (277)
$AlNH_3$	−298.068 46	$r_{AlN} = 2.35$; $r_{NH} = 1.02,1.03$	$\angle_{AlNH} = 108.8, 113.1$; $\angle_{HNH} = 107.9, 106.8$	3621.1 (40), 3620.7 (33), 1711.6 (46), 1257.3 (185)
H_2AlNH	−298.052 58	$r_{AlH} = 1.58$; $r_{AlN} = 1.79$; $r_{NH} = 1.01$	$\angle_{HAlN} = 120.2, 120.3$; $\angle_{AlNH} = 179.9$; $\angle_{HAlH} = 119.5$	3752.0 (67), 1996.9 (74), 1994.8 (239), 847.8 (353), 655.4 (358), 586.2 (70)
$AlNH_2$	−297.539 42	$r_{AlN} = 1.80$; $r_{NH} = 1.02$	$\angle_{AlNH} = 125.6$; $\angle_{HNH} = 108.8$	3653.9 (23), 1616.4 (66), 750.7 (90), 446.4 (276)
HAlNH	−297.455 05	$r_{AlH} = 1.56$; $r_{AlN} = 1.66$; $r_{NH} = 1.02$	$\angle_{HAlN} = 161.9$; $\angle_{AlNH} = 147.5$	3705.0 (90), 2078.3 (43), 506.7 (27), 317.0 (110)
HNAl[b]	−296.861 25	$r_{NH} = 1.02$; $r_{AlN} = 1.76$	$\angle_{HNAl} = 135.5$	3531.5 (3), 757.3 (17), 489.3 (365)
HAlN[b]	−297.661 79	$r_{AlH} = 1.55$; $r_{AlN} = 1.64$	$\angle_{HAlN} = 180.0$	2057.6 (12), 1079.5 (30), 481.2 (2x50)

[a] Inequivalent bonds. [b] Geometry and vibrational frequencies determined using the B3LYP/DFT method with 6-311G* basis set. The energy listed is from an MP2 calculation to provide for comparison with the other species in this table, but the MP2 calculation also yields imaginary vibrational frequencies for the bending mode.

TABLE 3: Observed and Calculated Vibrational Frequencies (cm^{-1}) for $AlNH_2$

	$AlNH_2$	$Al^{15}NH_2$	$AlND_2$	AlNHD
obs	3486.2	3477.4		
MP2	3653.9	3643.8	2691.0	3601.7, 2624.2
CCSD[a]	3660			
obs	1520.3	1514.9	1137.7	1348.8
MP2	1616.4	1611.1	1205.0	1429.2
CCSD[a]	1585			
obs	726.3	713.3	694.8	713.1
MP2	750.7	737.1	712.4	738.7
CCSD[a]	750			
obs	406.7	403.7		
MP2	446.4	443.4	346.9	399.8
CCSD[a]	413			

[a] Reference 1, using TZ2P basis set.

AlNHD peak in the mixed hydrogen isotope experiments, and this peak lies at 713.1 cm^{-1}.

$AlNH_2$ should also have a "scissors" motion of the NH_2 group, and according to MP2 calculations, this mode should be of nearly the same intensity as the Al−N stretch (Table 2), but with a smaller nitrogen isotopic shift. The 1520.3/1514.9 cm^{-1} pair of peaks has the same photolysis and annealing behavior as the Al−N stretch of $AlNH_2$ and is assigned to this scissors motion. The predicted 5.3 cm^{-1} shift nearly matches the observed 5.4 cm^{-1} shift, and the calculated frequencies are only 6.3−6.4% high. For $AlND_2$, the obvious counterpart is the sharp band at 1137.7 cm^{-1}, while the 1343.8 cm^{-1} band, strong in the NH_3/ND_3 experiments, represents this mode for AlNHD. Again, Table 3 presents the comparison between experiment and theory which is in accord with this assignment.

Although the Al−N stretch and NH_2 scissors are the two most prominent modes of $AlNH_2$ present in these experiments, the calculations predict that the strongest mode (by more than a factor of 3 over the next most intense mode; see Table 2) should occur at 446.4 cm^{-1} for $Al^{14}NH_2$ and 443.4 cm^{-1} for $Al^{15}NH_2$, with frequencies below 400 cm^{-1} for the AlNHD and $AlND_2$. Unfortunately, the instrument frequency range does not extend below 400 cm^{-1}, and the detector response near 400 cm^{-1} is much lower than in the middle of the spectral range. Nevertheless, an absorption at 406.7 cm^{-1} in the NH_3 experiment and a similar absorption at 403.7 cm^{-1} in the $^{15}NH_3$ experiment show approximately the same photolysis and annealing behavior as the other modes of $AlNH_2$ and are assigned to the out-of-plane motion of this molecule. The observed 3.0 cm^{-1} 14−15 shift matches the calculated value.

One final band observed for this molecule is the N−H asymmetric stretching mode at 3486.2 cm^{-1} with sites at 3476.8 and 3495.0 cm^{-1}. These absorptions are sufficiently seperated from the ammonia peaks as not to be ammonia cluster bands, but this is probably not the case for the deuterated counterparts, because no matching absorptions could be found. The ^{15}N absorption lies at 3477.4 cm^{-1} with sites at 3468.0 and 3486.6 cm^{-1}. The nitrogen 14/15 isotopic ratio, 1.002 53, is in good agreement with the calculated ratio, 1.002 77, for the N-H antisymmetric stretching mode.

Species 2: $HAlNH_2$. Although the Al−N stretching mode of $AlNH_2$ at 726.3 cm^{-1} is prominent in Figure 1a, the dominant species 2 product absorption lies at 704.6 cm^{-1} with a ^{15}N counterpart at 700.9 cm^{-1}. Such a small nitrogen isotopic shift compared to the nearby $AlNH_2$ peaks indicates that this mode is not due to an Al−N stretch. That the deuterium shift is far greater than that of $AlNH_2$ indicates that hydrogen plays a much larger role than nitrogen in this vibrational mode. Just as Davy and Jaffrey calculated the molecule $AlNH_2$ to be the most stable of the possible $AlNH_2$ isomers, they also calculated $HAlNH_2$ to be the most stable $AlNH_3$ isomer. $HAlNH_2$ has a calculated NH_2 rock at 770 cm^{-1} (765.7 cm^{-1} for the MP2 calculations). In the mixed hydrogen isotopic experiments (Figure 5b), there were several peaks of varying intensities with the same photolysis and annealing behavior. That there are five of such peaks between those of the NH_3 and ND_3 experiments indicates that there are at least three distinct hydrogens in this molecule and confirms the observation of $HAlNH_2$ with the structure calculated in ref 1. According to the previous and present *ab initio* calculations, $HAlNH_2$ is planar with three inequivalent hydrogens and a terminal NH_2 group. As a result, we have calculated eight distinct vibrational frequencies for the NH_2 rocking mode for all of the hydrogen isotopic combinations. These frequencies as well as those for other modes of this molecule are presented in Table 4. The intensity of the absorption depends largely on the isotope of the hydrogen bonded to the aluminum. This factor, combined with the abundance of deuterium relative to hydrogen in this experiment, accounts for the observed peak intensity distribution in Figure 5b, with only $HAlNH_2$ and $DAlNH_2$ not observed.

Both sets of calculations predict the Al−N stretching mode to occur less than 100 cm^{-1} higher in energy than the NH_2 rock.

TABLE 4: Observed and Calculated Vibrational Frequencies (cm^{-1}) for $HAlNH_2$

	$HAlNH_2$	$HAl^{15}NH_2$	$DAlND_2$	mixed H/D[a]
obs	1761.7	1761.7	1282.7	1761.7, 1282.7
MP2	1910.3	1910.3	1376.4	1375.8, 1910.2, 1910.2 1375.5, 1374.9, 1910.2
CISD[b]	1972			
obs	1524.9	1521.7	1151.4	1365.6, 1360.2
MP2	1626.4	1621.0	1214.1	1626.7, 1446.6, 1440.6 1447.1, 1441.6, 1214.6
CISD[b]	1627			
obs	778.7	766.9	748.3	749.2?
MP2	808.1	794.6	763.6	805.5, 796.2, 804.3 794.2, 798.6, 766.1
CISD[b]	836			
obs	704.6	700.9	549.8	655.5, 651.2, 644.2, 580.2, 575.0
MP2	765.7	760.7	594.9	718.7, 708.1, 693.8 634.5, 625.0, 683.4
CISD[b]	770			

[a] For MP2 calculated mixed H/D frequencies, the top row lists $DAlNH_2$ first, followed by both versions of HAlNHD. The bottom row lists DAlNHD first and second, followed by $HAlND_2$. [b] Reference 1, using the DZP basis set.

The peak at 778.7 cm^{-1}, with a matrix site at 785.3 cm^{-1}, seems to fit the description quite well. For the ^{15}N counterpart at 766.9 cm^{-1}, the nitrogen isotopic shift of 11.8 cm^{-1} compares favorably with the MP2 value of 13.5 cm^{-1}. For ND_3, the peak at 748.3 also tracks with these bands, and the 1.040 76 nitrogen isotopic ratio is less than the calculated value of 1.058 28 because of anharmonicity and the tendency of open-shell calculations to be a bit less reliable than their closed-shell counterparts. Unfortunately, ND_3 precursor absorptions preclude observation of mixed hydrogen isotopic modes. Nevertheless, the location of the assigned peaks in the Al−N stretching region, as well as isotopic shifts consistent with such a mode and similar photolysis and annealing behavior to other modes of the molecule, confirms the assignment.

One of the strongest modes of this molecule is the Al−H stretching mode, calculated at 1910.3 cm^{-1} for $HAl^{14}NH_2$. The absorption at 1761.7 cm^{-1} (with matrix site at 1739.8 cm^{-1}) tracks with the other peaks for this molecule and, as predicted by the calculations, does not shift perceptibly in the ^{15}N experiment. Upon deuteration, this mode shifts to 1282.7 cm^{-1} (with matrix site at 1269.4 cm^{-1}), and the isotopic ratio of 1.373 43 compares favorably with the theoretical prediction of 1.387 90. For mixed isotopic experiments, no intermediate peaks are observed, and the calculations predict this to be the case (Table 4).

As with $AlNH_2$, $HAlNH_2$ has a terminal H−N−H bending mode, and this occurs at 1524.9 cm^{-1}. For ^{15}N, this mode shifts to 1521.7 cm^{-1}. Both peaks increase on photolysis and decrease upon annealing to 25 K, as with the other $HAlNH_2$ modes. For $DAlND_2$ there are a few candidates near 1150 cm^{-1} for this band, but only the 1151.4 cm^{-1} absorption shows the proper postdeposition behavior. The 1149.4 and 1147.2 cm^{-1} bands are likely matrix sites of the $AlND_2$ peak at 1137.8 cm^{-1} and correspond to the $AlNH_2$ matrix sites at 1533.5 and 1537.7 cm^{-1}. MP2 calculations predict frequencies of 1626.4, 1621.0, and 1214.1 cm^{-1} for $HAl^{14}NH_2$, $HAl^{15}NH_2$, and $DAlND_2$, respectively, and the nitrogen and hydrogen isotopic ratios are in reasonable agreement with experiment (Table 4). For the mixed hydrogen isotopes, the calculated intermediate peaks lie between 1440 and 1450 cm^{-1}. Because the observed $HAlNH_2$ and $DAlND_2$ absorptions appeared at frequencies 6% lower than predicted, one expects to see intermediate peaks near 1360 cm^{-1}. In Figure 5b, weak absorptions at 1356.6, 1360.2, and 1365.6 cm^{-1} track reasonably well with the other bands and may be due to mixed isotopes, but due to the weakness of these peaks, a definitive assignment is not possible.

An EPR study of the reaction of ground state Al atoms with NH_3 in an adamantane matrix at 77 K suggested the $HAlNH_2$ molecule as a product but proposed bridging of one amine hydrogen to the aluminum atom.[9] Such a structure is not in agreement with the present and earlier[1,8] electronic structure calculations nor with the infrared observation of a terminal H−N−H "scissors" bending mode for this molecule. Furthermore, the strongest mode involving in-plane rocking of the AlH hydrogen, and the NH_2 hydrogens would be vastly different for the EPR structure from that calculated and observed here for seven isotopic molecules.

Species 3: HAlNH. The other reasonably intense absorption in the Al−H stretching region occurs at 1899.5 cm^{-1} with sites at 1890.9 and 1887.8 cm^{-1}. Unlike most other peaks in these experiments, this absorption increases strongly on annealing (Table 1). The trace of this product in the mixed H/D experiments suggests no more than two hydrogens for this molecule. Although it is calculated to be much less stable than the $AlNH_2$ isomer, HAlNH is the source of these absorptions, with the DAlND band at 1384.3 cm^{-1}. MP2 calculations predict HAlNH and DAlND absorptions at 2078.3 and 1507.6 cm^{-1}, respectively, with a hydrogen isotopic ratio of 1.378 55, in excellent agreement with the observed ratio of 1.372 17. For $HAl^{15}NH$, there is no predicted isotopic shift, as observed. For HAlND, the predictions give a shift of only 0.1 cm^{-1} from HAlNH, which is less than the resolution of the instrument and accounts for much of the observable intensity at 1899.5 cm^{-1} in the mixed H/D experiments. For DAlNH, the predicted frequency is only 0.7 cm^{-1} higher than for DAlND and accounts for the breadth of the nominal 1384.3 cm^{-1} peak in the mixed H/D experiments.

Although we could not observe the strongest predicted mode (above 400 cm^{-1}) of this molecule, the N−H stretch calculated at 3705.0 cm^{-1} (Table 2) is probably masked by ammonia and ammonia cluster absorptions.[19] The Al−H stretch calculates as the second most intense absorption in the observable region, and the third is the linear bend of the hydrogens toward each other (i.e., one rotating counterclockwise, while the other rotates clockwise). For $H^{14}AlNH$, this mode is predicted at 506.7 cm^{-1} and has a 0.6 cm^{-1} ^{15}N shift. In the experiment, a mode at 530.6 cm^{-1}, with ^{15}N counterpart at 530.5 cm^{-1}, matches the calculations reasonably well and tracks with the Al−H stretch of this molecule. Although MP2 calculations usually overestimate vibrational frequencies, they occasionally underestimate bending modes.[20] Reference 1 reported this bending mode at 498 cm^{-1}, in very close agreement with the MP2 results and still 6.5% lower than the observed value. For DAlND, the predicted frequency for this mode is at 367.8 cm^{-1}, but no corresponding peak could be observed in the low signal-to-noise region just above 400 cm^{-1}. In the mixed H/D experiments, however, two absorptions that upon photolysis and annealing behave like the 530.6 cm^{-1} peak appear at 495.5 and 489.6 cm^{-1}, the former more intense than the latter. The linear bend of HAlND is predicted at 449.5 cm^{-1}, and the same mode calculates at 455.2 cm^{-1} for DAlNH, with the latter (i.e., higher frequency) mode having a calculated intensity of 40 km mol^{-1} vs 26 km mol^{-1} for the former, in rough agreement with experiment. Although the observed frequency shift between HAlNH and DAlNH is 30% lower than predicted, the shift between DAlNH and HAlND is quite close to the calculations,

and the postdeposition behavior of these absorptions tracks them with the Al−H bands of HAlNH.

In reactions of boron with ammonia, HBNH was the major product, and the identification of BNH_2 was tenuous.[5] With the larger aluminum atom, however, $AlNH_2$ is a major product and is calculated by MP2 to be 52.9 kcal mol^{-1} (40.9 kcal mol^{-1} in ref 1) more stable than HAlNH. Also, unlike HBNH, HAlNH is calculated by both methods to be trans-planar, not linear. This seems to indicate that the formation of HXNH compared to XNH_2, where X is either Al or B, is different for each of the group III atoms.

Purely on the basis of thermodynamics, then, despite the prominence of HBNH in the boron−ammonia experiments, one might not expect any observable HAlNH in the present spectra. Nevertheless, Davy and Jaffrey also calculated a high interconversion barrier (72.4 kcal mol^{-1}) between the two. Thus, some HAlNH forms via the reaction of energetic Al atoms and relaxes before conversion to $AlNH_2$. The strong barrier to interconversion keeps the two products from equilibrating (i.e., forming more $AlNH_2$ at the expense of HAlNH) during the matrix condensation process. On annealing HAlNH can form by diffusion and combination of AlH and NH fragments.

Species 4 and 5: $Al(NH_2)_2$ and $Al(NH)_2$. In Figure 1, two sets of peaks form nitrogen isotopic triplets, indicative of products with two identical nitrogen atoms. That these two products do not appear in the ND_3 experiments indicates that they each possess at least one hydrogen atom. Therefore, the likely products would be aluminum bonded to two ammonia molecules or two identical ammonia fragments. For $AlNH_3$, both ref 1 and our calculations indicate that the Al−N bond is weak and that the absorption should occur at 200 cm^{-1} (ref 1) or 237.6 cm^{-1} (MP2). Al−N bonds are stronger (formally double bonds) in $AlNH_2$ than in $AlNH_3$, and the reported value of 726.3 cm^{-1} for the Al−N stretch is in accord with this. MP2 calculations on $Al(NH_2)_2$ yield two low imaginary frequencies, but the remaining frequencies are in accord with what would be expected of such a product given the results for $AlNH_2$. The strongest calculated observable peak occurs at 806.8 cm^{-1} with one nearly equally as strong at 1622.0 cm^{-1}. For $Al(^{14}NH_2)(^{15}NH_2)$, these peaks shift to 801.4 and 1619.0 cm^{-1}, respectively, and shift further to 795.4 and 1617.2 cm^{-1} for $Al(^{15}NH_2)_2$. The observed triplet at 747.7, 742.3, and 737.5 cm^{-1} matches these calculations well, as each is 7.3−7.4% lower than predicted. For the upper mode, the broad collection of peaks at 1541 cm^{-1}, which shifts to approximately 1537 cm^{-1}, fits the calculation reasonably well and is tentatively assigned to the NH_2 scissors motions of $Al(NH_2)_2$.

For the triplet at 833.1, 827.2, and 821.4 cm^{-1} (plus blue matrix sites for each), one should anticipate a stronger Al−N bond. Because aluminum can form stronger bonds with nitrogens when there are fewer hydrogens attached, $Al(NH)_2$ seems a likely choice. Although calculations for this radical also yield negative frequencies for some of the lower frequency modes, the prediction of an Al−N stretch at 905.3 cm^{-1} (8.7% higher than experiment) seems quite reasonable. This mode is predicted to be the most intense absorption. The predictions for $Al(^{14}NH)(^{15}NH)$ and $Al(^{15}NH)_2$ are 898.6 cm^{-1} (+8.6%) and 891.8 cm^{-1} (8.6%), respectively. It is interesting to note that a trace of HNNH was detected in these experiments.[21]

Other Bands and Potential Products. The peak at 1958.4 cm^{-1} in the Al−H stretching region and the matching Al−D peak at 1436.1 cm^{-1} are both nearly destroyed upon photolysis, suggesting an unstable product with an Al−H stretch. In the mixed H/D experiments, both of these peaks can be seen with an approximate 2:1 ratio between the Al−D and Al−H stretching modes, suggesting further that this unstable product has a single hydrogen. On the basis of this information, then, it seems that this product might be HAlN, which has B3LYP calculated frequencies of 2057.6 and 1496.3 cm^{-1} for HAlN and DAlN, respectively. Both the Al−N stretching mode, calculated at 1079.5 cm^{-1}, and the degenerate bending mode at 481.2 cm^{-1} are calculated to be more intense than the Al−H stretch, but no evidence of these modes is observed. Table 2 also suggests that HNAl should be far more stable than HAlN, because N-H bonds are stronger than Al−H bonds, but no evidence for HNAl is found. It may be that the mechanism for forming HAlN (e.g., AlH bashing ammonia fragments while in the hot laser plume) is much more facile than that for HNAl, and it is then trapped effectively before declining precipitously upon photolysis. Nevertheless, because of the absence of the lower frequency modes, a definite assignment of HAlN cannot be made.

The other curious absorptions are the doublets at 1799.2 and 1800.6 cm^{-1} for NH_3 experiments and 1797.9 and 1799.4 cm^{-1} for ND_3 experiments. Their enormous growth on annealing indicates that they may be aggregates of some kind. The small hydrogen isotope shift indicates that this cannot be an Al−H stretching mode. Because the level of impurity in the system was very low, this peak must be of a product with only Al, N, and H. The small isotope shift, then, is more suggestive of an electronic transition of an aggregate, with the isotope shift due the difference in zero-point energy.

Few, if any, other higher order products were detected in the experiments. Although calculated to be not much less stable than $HAlNH_2$, there is no evidence for $AlNH_3$ or H_2AlNH in the spectra. According to the MP2 calculations, $AlNH_3$ should have its strongest absorption at 1257.3 cm^{-1}, with a 6.6 cm^{-1} nitrogen shift and a 301.4 cm^{-1} hydrogen shift. Small peaks at 1195.2 and 1189.3 cm^{-1} for ^{14}N and ^{15}N, respectively, may correspond to $AlNH_3$, but the lack of information on other modes, due mainly to overlap with parent NH_3 modes, prevents any positive identification. The Al−N stretch of this species is very weak, calculated at 237.6 cm^{-1}, and not observable in these experiments. For H_2AlNH, MP2 calculations predict that there should be two dominant absorptions at 655.4 cm^{-1} (with a 0.9 cm^{-1} ^{15}N shift) and 847.8 cm^{-1} (with a 1.0 cm^{-1} ^{15}N shift). Nothing in the spectra is consistent with these predictions. Calculations on higher order molecules, such as AlNAlH, H_2NAlH_2, and H_2NAlNH, are also not consistent with the experimental data. Finally, if the higher $Al(NH_3)_x$ complexes suggested by the EPR study[9] were produced here, their infrared spectra could not be distinguished from unreacted NH_3 precursor absorptions.

Reaction Mechanisms. Some comments on the reaction mechanism are appropriate. The marked growth of $AlNH_2$ and $HAlNH_2$ absorptions on broad-band photolysis (240−580 nm) and the decrease on annealing show that electronically excited Al atoms are required for the insertion reaction. This is in agreement with earlier studies on the reaction of Al atoms with H_2 and with CH_4.[17,22,23] The excited $(HAlNH_2)^*$ species formed during condensation with translationally/electronically hot[16,17] Al atoms can eliminate H, AlH, NH_2, or NH to form products or be collisionally quenched by the condensing argon matrix, thus trapping the insertion product $HAlNH_2$ molecule which is identified here.

Conclusions

This article has presented experimental and computational evidence for at least three new products containing aluminum, nitrogen, and hydrogen. The major reaction products are

$HAlNH_2$ and $AlNH_2$. The minor products, HAlNH and possibly HAlN, are detected in the argon matrix despite having much more stable isomeric forms. By contrast, some molecules, such as H_2AlNH, do not appear in the spectra despite having calculated energies near those of observed products. Three interesting differences are found with boron−ammonia reaction products. The primary insertion product with aluminum, $HAlNH_2$, is trapped in large yield whereas decomposition to the linear HBNH molecule was favored with boron; in contrast, the major decomposition product was $AlNH_2$ with aluminum. Finally, no evidence was found for secondary aluminum reaction products, whereas BNBH was a major product in boron−ammonia experiments.[4,5]

For the most part, MP2 calculations are comparable to the more sophisticated CISD and CCSD calculations of Davy and Jaffrey,[1] especially for the major products $AlNH_2$ and $HAlNH_2$ observed here. Such results should allow further work on III−V compounds with the present experimental arrangement using laser ablation and matrix isolation spectroscopy supported by reliable and relatively inexpensive computations.

Acknowledgment. We gratefully acknowledge support from the Air Force Office of Scientific Research under Grant F49620-97-1.

References and Notes

(1) Davy, R. D.; Jaffrey, K. L. *J. Phys. Chem.* **1994**, *98*, 8930.
(2) Hassanzadeh, P.; Andrews, L. *J. Am. Chem. Soc.* **1992**, *114*, 9239.
(3) Hassanzadeh, P.; Hannachi, Y.; Andrews, L. *J. Phys. Chem.* **1993**, *97*, 6418.
(4) Thompson, C. A.; Andrews, L. *J. Am. Chem. Soc.* **1995**, *117*, 10125.
(5) Thompson, C. A.; Andrews, L.; Martin, J. M. L.; El-Yazal, J. *J. Phys. Chem.* **1995**, *99*, 13839.
(6) Lanzisera, D. V.; Andrews, L. *J. Phys. Chem. A* **1997**, *101*, 824.
(7) Fink, W. H.; Richards, J. C. *J. Am. Chem. Soc.* **1991**, *113*, 3393.
(8) Sakai, S. *J. Phys. Chem.* **1992**, *96*, 8369.
(9) Howard, J. A.; Jolly, H. A.; Edwards, P. P.; Singer, R. J.; Logan, D. E. *J. Am. Chem. Soc.* **1992**, *114*, 474.
(10) Gaussian 94, Revision B.1: Frisch, M. J.; Trucks, G. W.; Schlegel, H. B.; Gill, P. M. W.; Johnson, B. G.; Robb, M. A.; Cheeseman, J. R.; Keith, T.; Petersson, G. A.; Montgomery, J. A.; Raghavachari, K.; Al-Laham, M. A.; Zakrzewski, V. G.; Ortiz, J. V.; Foresman, J. B.; Cioslowski, J.; Stefanov, B. B.; Nanayakkara, A.; Challacombe, M.; Peng, C. Y.; Ayala, P. Y.; Chen, W.; Wong, M. W.; Andres, J. L.; Replogle, E. S.; Gomperts, R.; Martin, R. L.; Fox, D. J.; Binkley, J. S.; Defrees, D. J.; Baker, J.; Stewart, J. P.; Head-Gordon, M.; Gonzalez, C.; Pople, J. A. Gaussian, Inc., Pittsburgh, PA, 1995.
(11) Head-Gordon, M.; Pople, J. A.; Frisch, M. *Chem. Phys. Lett.* **1988**, *153*, 503. Frisch, M. J.; Head-Gordon, M.; Pople, J. A. *Chem. Phys. Lett.* **1990**, *166*, 275. Frisch, M. J.; Head-Gordon, M.; Pople, J. A. *Chem. Phys. Lett.* **1990**, *166*, 281.
(12) Dunning, T. H., Jr.; Hay, P. J. In *Modern Theoretical Chemistry*; Schaefer, H. F. III, Ed.; Plenum: New York, 1976; pp 1−28.
(13) Schlegel, H. B. *J. Comput. Chem.* **1982**, *3*, 214.
(14) Stevens, P. J.; Devlin, F. J.; Chablowski, C. F.; Frisch, M. J. *J. Phys. Chem.* **1994**, *98*, 11623.
(15) McLean, A. D.; Chandler, G. S. *J. Chem. Phys.* **1980**, *72*, 5639. Krishnan, R.; Binkley, J. S.; Seeger, R.; Pople, J. A. *J. Chem. Phys.* **1980**, *72*, 650. Wachters, A. J. H. *J. Chem. Phys.* **1970**, *52*, 1033. Hay, P. J. *J. Chem Phys.* **1977**, *66*, 4377. Raghavachari, K.; Trucks, G. W. *J. Chem. Phys.* **1989**, *91*, 1062.
(16) Andrews, L.; Burkholder, T. R.; Yustein, J. T. *J. Phys. Chem.* **1992**, *96*, 10182.
(17) Chertihin, G. V.; Andrews, L. *J. Phys. Chem.* **1993**, *97*, 10295.
(18) Milligan, D. E.; Jacox, M. E. *J. Chem. Phys.* **1965**, *43*, 4487.
(19) Suzer, S.; Andrews, L. *J. Chem. Phys.* **1988**, *89*, 5347.
(20) Lanzisera, D. V.; Andrews, L. *J. Phys. Chem. A* **1997**, *101*, 1482.
(21) Minkwitz, R. *Z. Anorg. Allg. Chem.* **1974**, *1*, 411. Rosengren, K.; Pimentel, G. C. *J. Chem. Phys.* **1965**, *43*, 507.
(22) Pullumbi, P.; Mijoule, C.; Manceron, L.; Bouteiller, Y. *Chem. Phys.* **1994**, *185*, 13.
(23) Parnis, J. M.; Ozin, G. A. *J. Phys. Chem.* **1989**, *93*, 1215.